

# Mixed signal processing and machine learning methods for bearings fault detection: Application in predictive meaintenance (Project outline)

Yapi Donatien Achou

February 18, 2019

## Contents

<b>1</b>	<b>Introduction</b>	<b>2</b>
<b>2</b>	<b>Preview work</b>	<b>3</b>
<b>3</b>	<b>Signal processing methods</b>	<b>3</b>
3.1	Overview . . . . .	3
3.2	Fourier transform . . . . .	4
3.2.1	Theory . . . . .	4
3.2.2	Application . . . . .	4
3.3	Wavelet transform . . . . .	9
3.3.1	Theory . . . . .	9
3.3.2	Application . . . . .	9
3.4	Hilbert Huang transform . . . . .	11
3.4.1	Theory . . . . .	11
3.4.2	Application for bearings fault detection . . . . .	13
<b>4</b>	<b>Machine learning methods</b>	<b>17</b>
4.1	Overview . . . . .	17
<b>5</b>	<b>Result</b>	<b>17</b>
5.1	Overview . . . . .	17
<b>6</b>	<b>Conclusion</b>	<b>17</b>

# 1 Introduction

Predictive maintenance can be defined as a maintenance philosophy with a set of methods used to predict and prevent machine failure in order to avoid unexpected downtime. This maintenance philosophy when correctly implemented, increases machine life time, and reduces maintenance cost [referecne].

In rotating machines, more than 40 % of machine malfunction can be attributed to bearing defect [references].

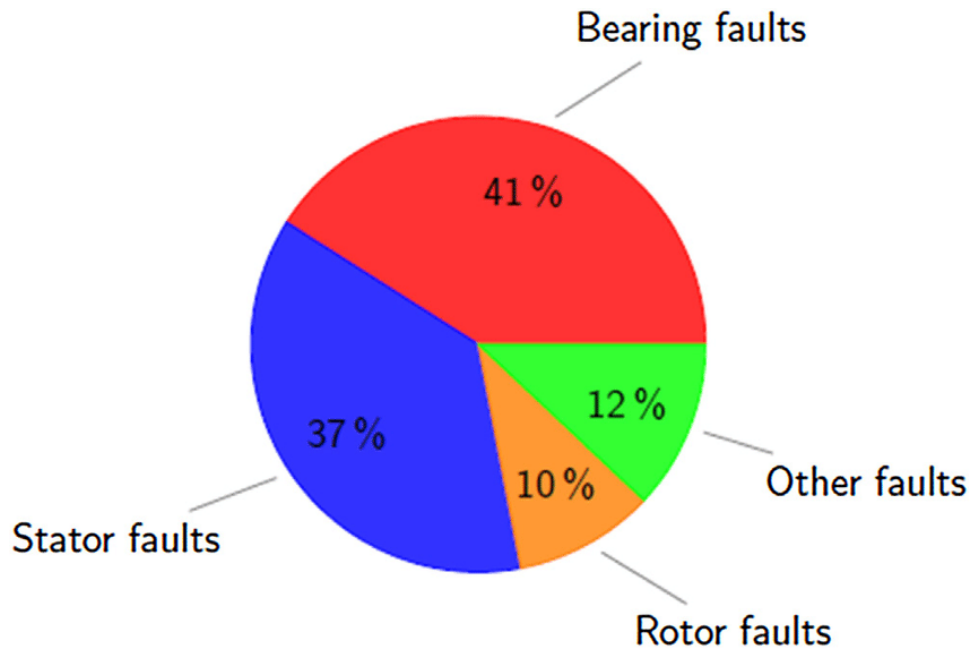


Figure 1: Defect statistic, taken from [reference]

In this project we present a mixed methodology to detect and predict bearing defects. The methodology consists of using signal processing for feature generation and data labelling, and machine learning for defects classification and failure prediction. For a given input dataset, the dataset is decomposed into its subcomponents or basis components. The basis components also called features are then used as input of a supervised learning algorithm for defect classification and failure prediction.

The signal processing methods used are Fourier transform, wavelet transform and Hilbert Huang transform. We focus on ensemble learning and feed forward neural network for classification. Furthermore we show that the back-propagation process in the feed

forward neural network can be modelled by an ordinary differential equation, whose solution represents the path of the hidden and output layer weights.

The outline of the project is as followed: In section (chapter) one we give an overview of the signal processing methods. In section (chapter) two we present the machine learning methodology and show that the back-propagation in the feedforward neural network can be modelled as a differential equation. In section (chapter) 3 we present a case study where we apply the methodology defined in section one and two. In section four we present the conclusion of this work.

## 2 Preview work

## 3 Signal processing methods

### 3.1 Overview

We present three signal processing methods for data decomposition or feature generation. The three methods can be described as follow: Given a time series approximated by a map

$$f : \mathbb{R} \rightarrow \mathbb{R}, \quad (1)$$

find a a basis  $\{\varphi_j\}_{j=0}^n$  that span a vector space  $V$  such that

$$f(x) = \sum_{j=0}^{j=n} \alpha_j \varphi_j. \quad (2)$$

In the context of this work, the basis functions  $\{\varphi_j\}_{j=0}^n$  are the features derived from the original dataset. Furthermore, we show that the derived feature(s) contain enough information about the map  $f$ . In practical sense, this information could be defect information for a time series from a broken machine or equipment.

To illustrate the methods, we apply each method on a case study.

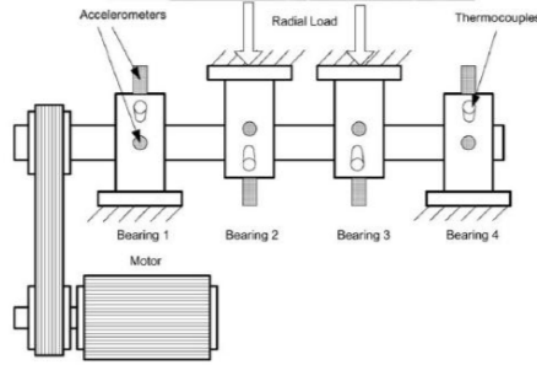


Figure 2: Experimental set up

The data used in this use case was generated by the Intelligence Maintenance system (IMS) [reference]. Three separate experiments involving four bearings were performed on a motor. In each experiment, a 1-second vibration signal snapshots was recorded every 10 minutes, for a specified time. Each vibrational signal sample consists of 20 480 data points with sampling rate of 20 000 Hz.

## 3.2 Fourier transform

### 3.2.1 Theory

### 3.2.2 Application

In this approach we use Fourier transform to detect defect frequency such outer race defect frequency and inner race defect frequency in the envelop spectrum. In this case the envelop spectrum is the new feature generated from the original vibration data. The bearing type used are Rexnor ZA-2115. For this type of bearing, the constant defect frequency (cdf) for ball pass frequency outer race defect is 0.1182 and the constant defect frequency for ball pass frequency inner race defect is 0.1484 [reference]. According to Rexnord product engineering group [reference], to find the defect frequency in Hz we multiply the constant defect frequency (cdf) by the rotational speed of the bearing ( here 2000 RPM), to find the defect frequency in Hz. Note that the defect frequency is computed from the geometry of the bearing, which means that for a specific bearing, this is a constant value.

Figure 3 shows the geometry of a bearing, from which bearing defect frequency can be computed. Figure 4 illustrates how Fourier transform can decompose vibration data into its frequency components. Each frequency component which are trigonometric functions are characterised by constant frequency and amplitude. In a defect bearing, the defect frequency will be coupled with a relatively high amplitude.

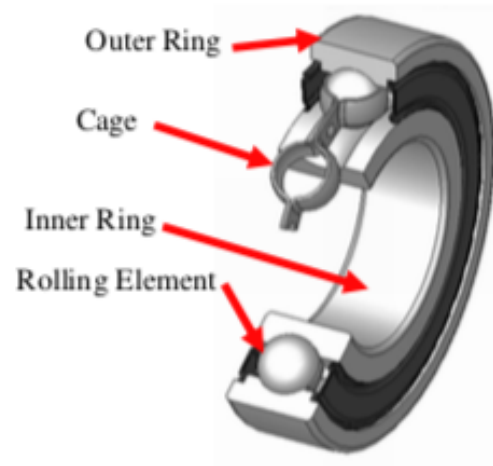


Figure 3: Geometry of a bearing

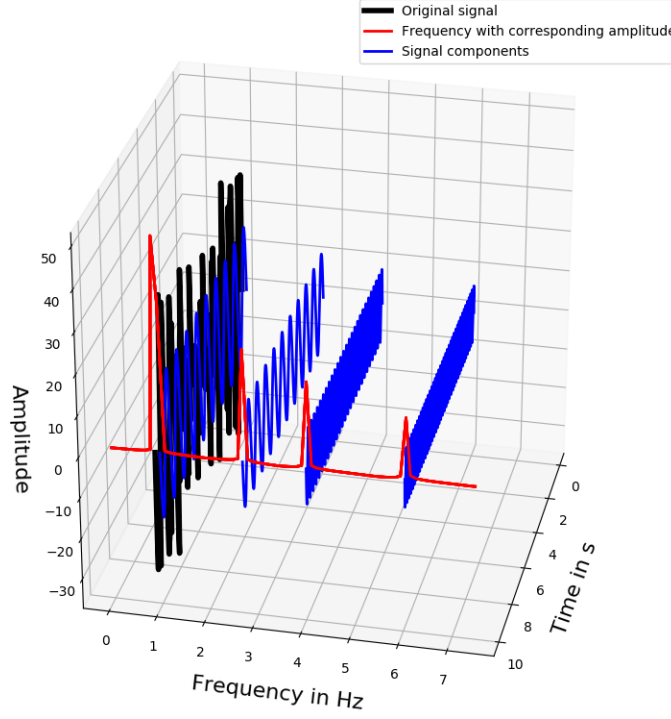


Figure 4: Illustration of using Fourier transform to decompose a time signal to its frequency components

Next, we compute the envelop spectrum for each vibration signal by using the FFT method (Fast Fourier Transform). The envelop spectrum is used to detect early sign of failure. Recall that a vibration signal can be decomposed into its sub components, where each sub component is characterised by its frequency and its amplitude. Early sign of failure can be seen in the high frequency low amplitude sub component. As the failure becomes more pronounced, it becomes visible in the low frequency high amplitude sub component. Figure 5 shows the raw vibration signal, the corresponding envelop spectrum and the ball pass frequency outer race defect.

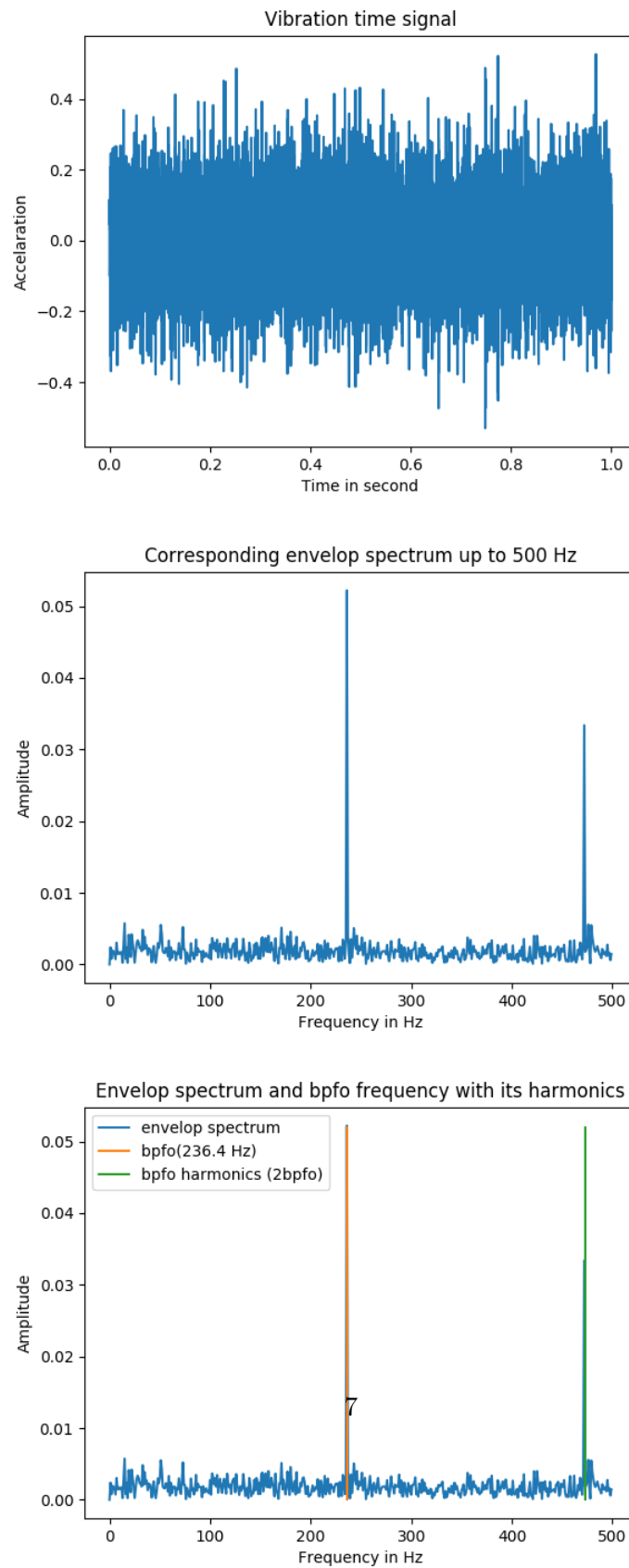


Figure 5: Vibration time signal

By computing the envelop spectrum for each time signal and extracting the amplitude of a defect frequency we can visualise the severity of a defect. Figure 6 and ?? show the amplitude of outer race defect and inner race defect for four bearings and three bearings respectively. In Figure 6 we can observe that bearing number one is affected severely by ball pass frequency outer race defect. Figure 7 shows that bearing number three has ball pass frequency inner race defect.

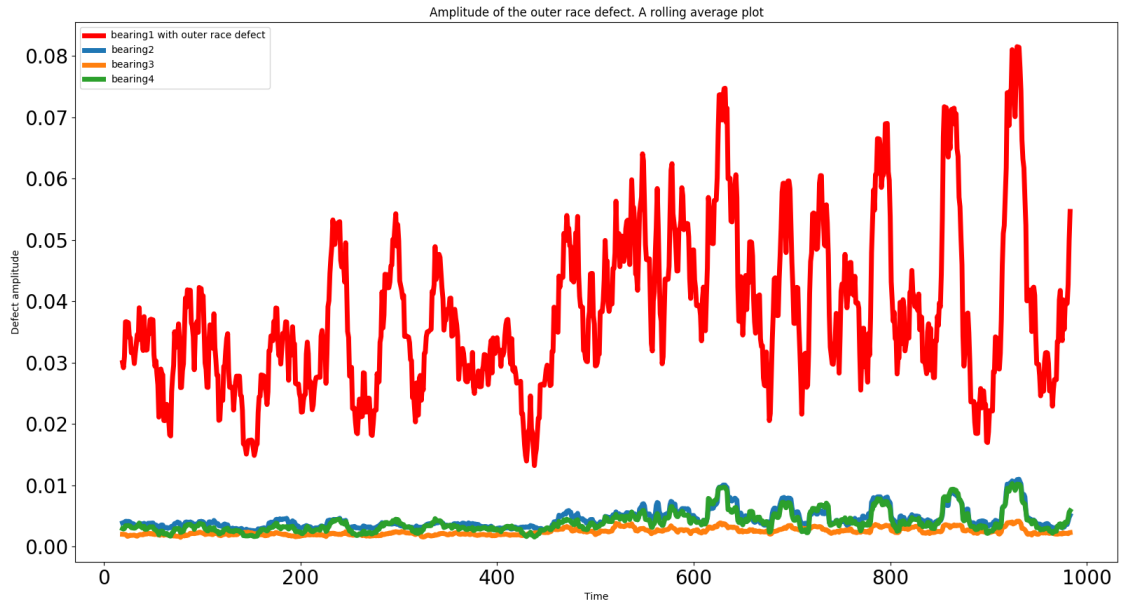


Figure 6: Ball pass frequency outer race detection



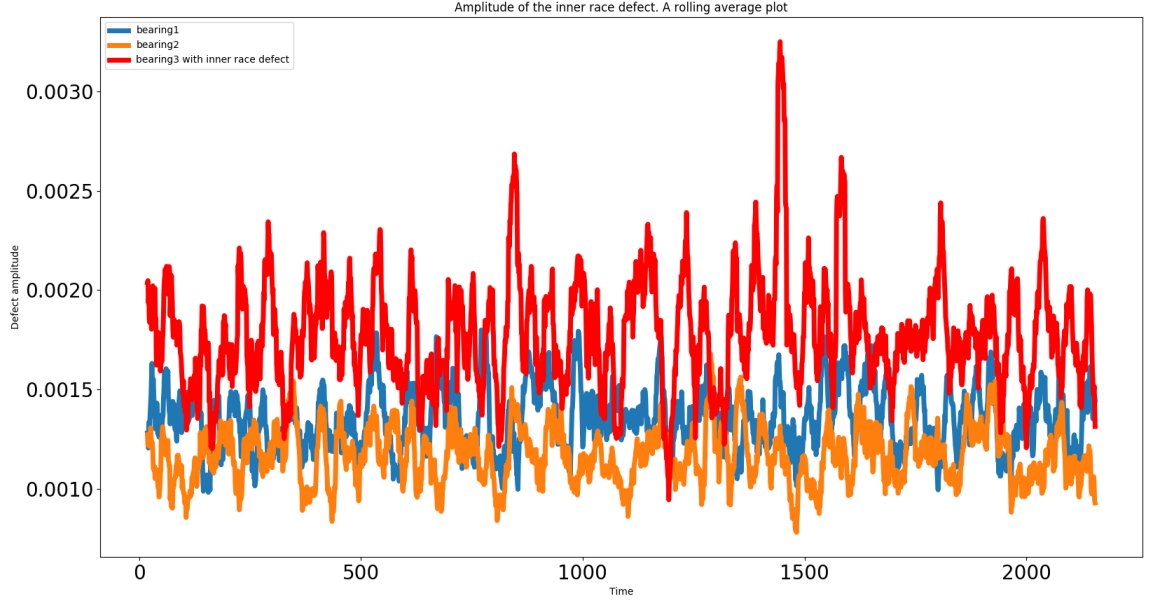


Figure 7: Ball pass frequency inner race detection

### 3.3 Wavelet transform

#### 3.3.1 Theory

#### 3.3.2 Application

In the wavelet transform we generate two extra features from the vibration time signal, namely the discrete detailed coefficient  $cD$  and the approximate coefficient  $cA$ . The detail coefficient  $cD$  represents the high frequency component of the vibration time signal and the approximate coefficient  $cA$  represents the low frequency component. For the mother wavelet we use Daubechies 20 or  $db20$  shown in Figure 8

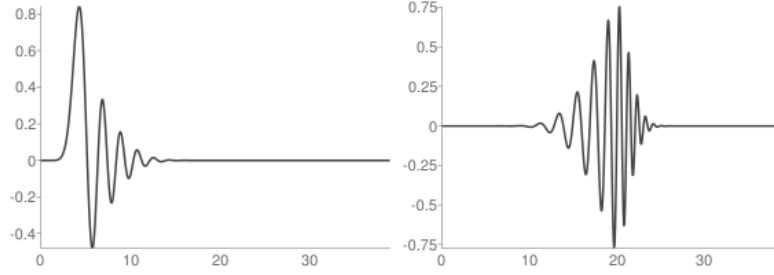


Figure 8: The scaling function  $\varphi$  (left) and the wavelet function  $\Psi$  (right)

Once we have the two extra features, we compute the dissimilarity between a reference sample and subsequent samples for each feature. This process generates a set of points  $(x, y)$  that represent the health index of each sample. From Figure 9 and 10, we can observe that bearing number four and bearing number three suffer from ball pass frequency outer race and ball pass frequency inner race defect respectively. We can also observe that a bearing can go through three main stages:

1. A healthy stage characterised by a low health index
2. A warning stage characterised by an increasing health index
3. An alarm stage characterised by a high health index

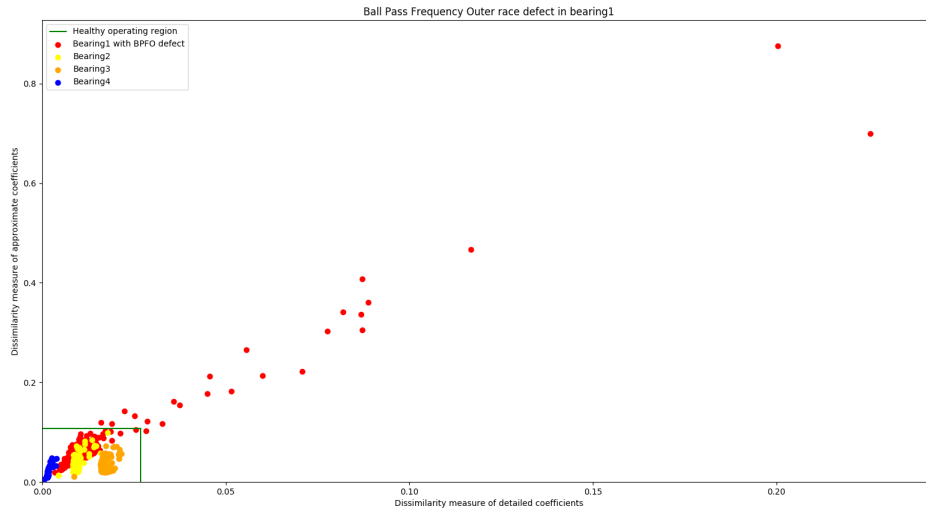


Figure 9: Ball past frequency outer race defect detection from wavelet transform

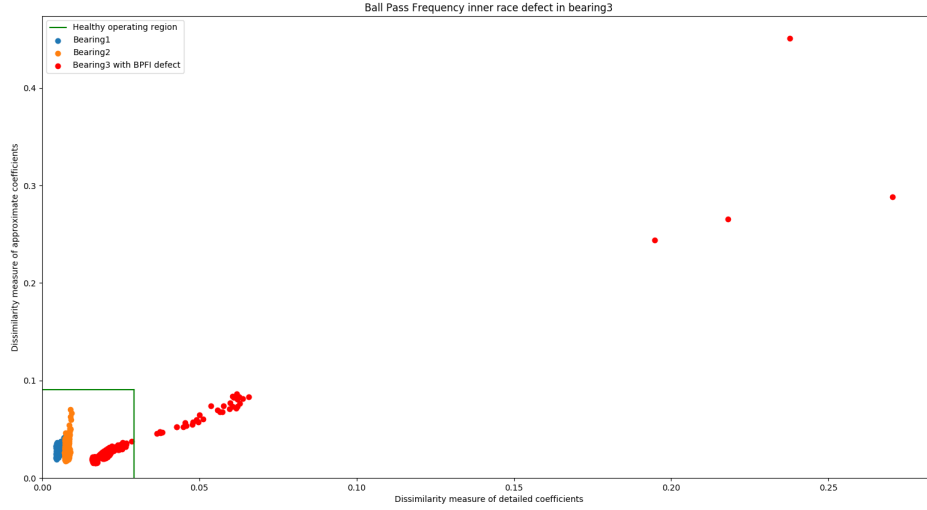


Figure 10: Ball past frequency outer race defect detection from wavelet transform

In the alarm stage, as the degradation becomes more severe, the distance between the points increases.

### 3.4 Hilbert Huang transform

#### 3.4.1 Theory

The Hilbert-Huang transform is a data decomposition methods that consists of decomposing data in an adaptive fashion. Adaptivity means that rather than imposing an a priori basis such as trigonometric functions, a posteriori basis functions are derived from the data itself [1]. In doing so, the method deals better with nonlinearity and non stationarity which are inherently present in real world data.

This method gives an alternative approach of time-frequency-energy paradigm by using Hilbert spectral analysis and the so call empirical mode decomposition (EMD) to express the nonlinearity and the non stationary in data with instantaneous frequency and instantaneous amplitude [1].

The empirical mode decomposition (EMD) originated from the quest of functions that can be expressed by a time-frequency-amplitude expression, such that the frequency is physically meaningful. Consider a time series  $x(t)$ . Its Hilbert transform  $H(t)$  is given by

$$H(t) = \frac{1}{\pi} P \int_{-\infty}^{\infty} \frac{x(\tau)}{t - \tau} d\tau, \quad (3)$$

where  $P$  is the Cauchy principal value. The corresponding time-frequency-amplitude function of  $x(t)$  is the analytical function

$$z(t) = x(t) + iy(t) = a(t)e^{i\theta(t)}, \quad (4)$$

where the instantaneous amplitude  $a(t)$  and phase  $\theta(t)$  can be computed by

$$a(t) = \sqrt{x(t)^2 + y(t)^2} \quad (5)$$

$$\theta(t) = \tan^{-1} \left( \frac{y(t)}{x(t)} \right). \quad (6)$$

Furthermore, the instantaneous frequency  $w(t)$  can be derived from the phase  $\theta(t)$  as

$$w(t) = \frac{d\theta}{dt}. \quad (7)$$

By setting

$$f(t) = \frac{y(t)}{x(t)},$$

the expression of the instantaneous amplitude  $w(t)$  in (7) can be expanded as

$$w(t) = \frac{f'(t)}{1 + f(t)^2} = \frac{y'(t)x(t) - y(t)x'(t)}{x(t)(x(t) + y(t)^2)}. \quad (8)$$

The instantaneous frequency  $w(t)$  using the Hilbert transform is not always physically meaning. For example for an arbitrarily function, the instantaneous physical frequency values should be positive. However this is not always the case.

For example if

$$f(x) = \cos(ct) + d \quad (9)$$

where  $c$  and  $d$  are constants, the instantaneous frequency is given by

$$w(t) = \frac{-c \sin(ct)}{1 + (\cos(ct) + d)^2} \quad (10)$$

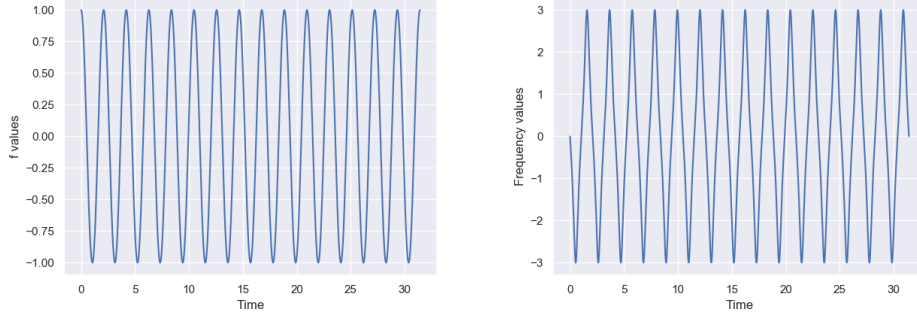


Figure 11: function  $f$  and its corresponding frequency

From Figure 11, we see that the instantaneous frequency takes negative values, which is not physically meaning full.

To circumvent this, the Hilbert-Huang transform offers a methodology to obtain from an arbitrarily function or time series  $x(t)$  a set of finite subcomponents whose instantaneous frequency are physically meaningful. This methodology let to the empirical mode decomposition.

The necessary condition for obtaining a physical frequency is that  $x(t)$  satisfies the approximate local envelope symmetry condition [2].

This condition is expressed in the empirical mode decomposition (EMD) such that an arbitrarily time series  $x(t)$  can be decomposed by a sifting process into intrinsic mode function  $c_i$

$$x(t) = \sum_{i=1}^n c_i + r_n \quad (11)$$

where the  $c_i$  satisfies the approximate local envelope symmetry condition

$$SD_k = \frac{\sum_{t=0}^T}{\sum_{t=0}^T} < \epsilon \quad (12)$$

where  $\epsilon$  is a small predefined real number.

### 3.4.2 Application for bearings fault detection

we consider a vibration signal with sample frequency of 20000Hz rotating speed of 2000 RPM

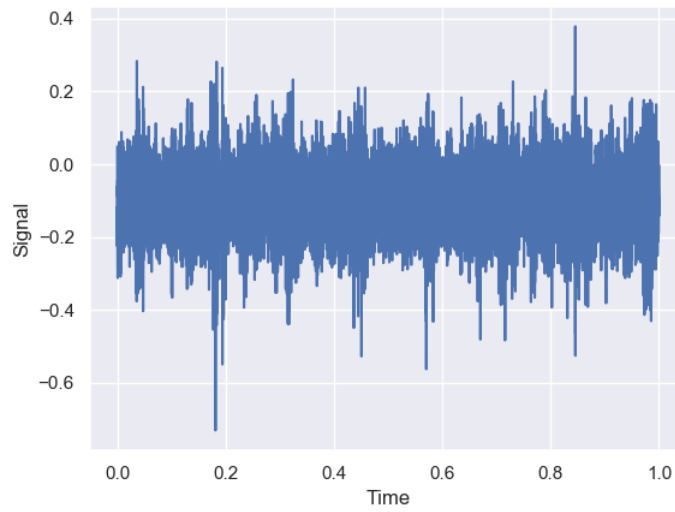


Figure 12: Vibration signal of 1 second snapshot

After applying the empirical mode decomposition on the vibration data from figure 12 we get sixteen intrinsic mode functions

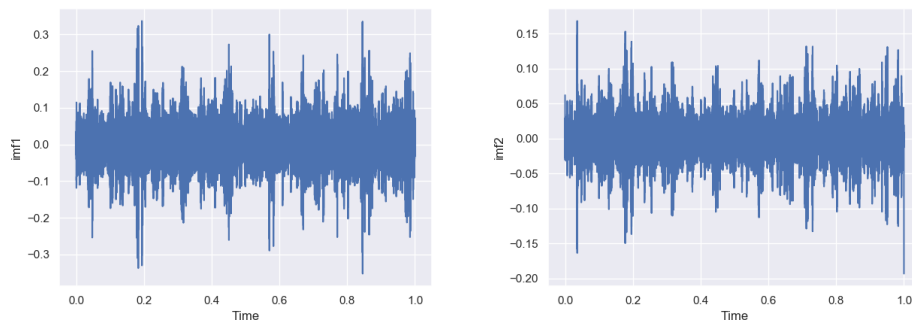


Figure 13: 1th and 2nd intrinsic mode function (imf)

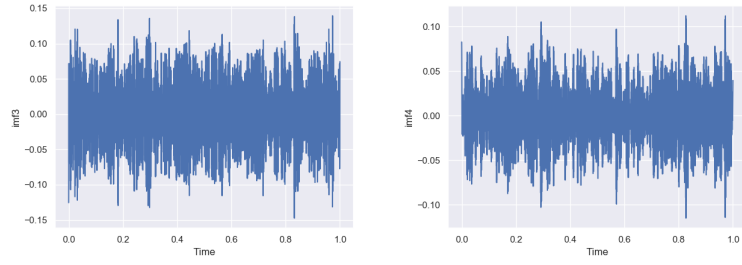


Figure 14: 3rd and 4th intrinsic mode function (imf)

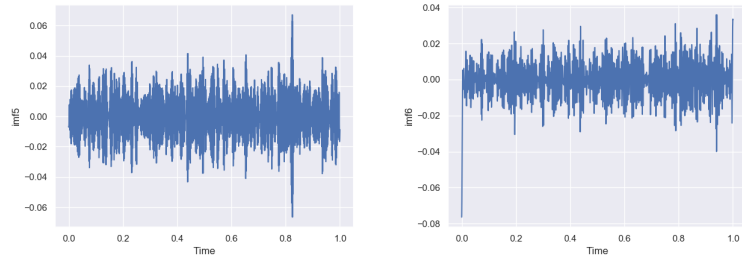


Figure 15: 5th and 6th intrinsic mode function (imf)

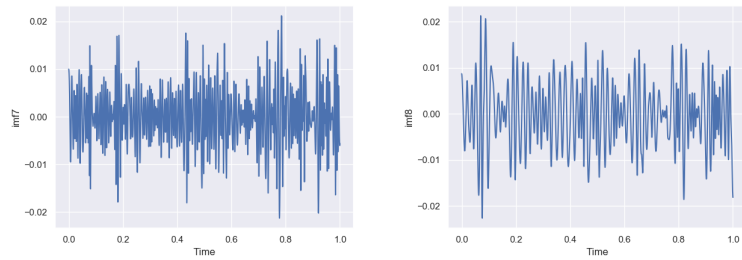


Figure 16: 7th and 8th intrinsic mode function (imf)

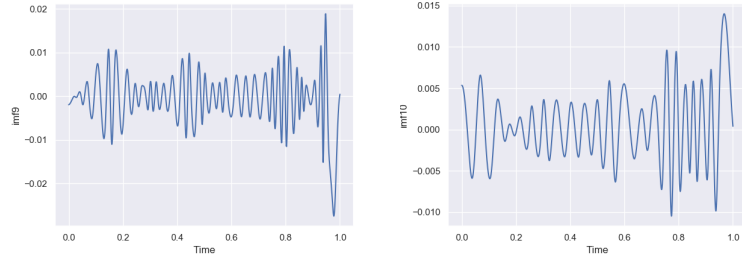


Figure 17: 9th and 10th intrinsic mode function (imf)

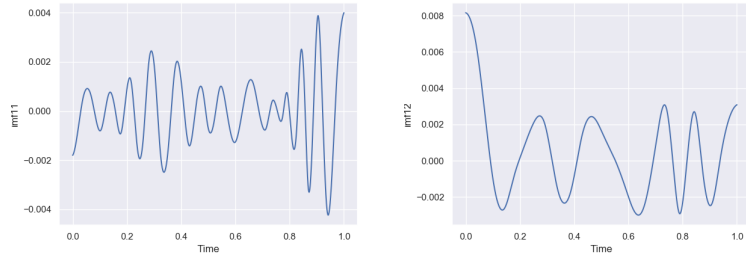


Figure 18: 11th and 12th intrinsic mode function (imf)

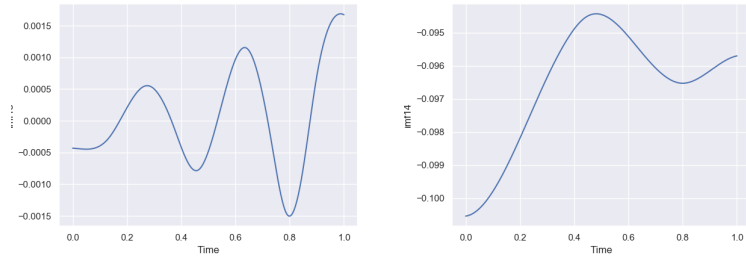


Figure 19: 13th and 14th intrinsic mode function (imf)



## 4 Machine learning methods

### 4.1 Overview

## 5 Result

### 5.1 Overview

## 6 Conclusion

## References

- [1] Norden E. Huang and Zhaohua Wu *A review on Hilbert-Huang Transform: Methods and its Application to Geophysical Studies*. Review of Geophysics, 2008
- [2] Norden E. Huang, Zheng Shen, Steven R. Long, Manlic C. Wu, Hsing H. Shih, Quanan Zheng, Nai-Chyuan Yen, Chi Chao Tung and Henry H. Liu *The Empirical mode decomposition and the Hilbert Spectrum for nonlinear and non-stationary time series analysis* Proc. R. Soc. Lond. A (1998) 455, 903:995.
- [3] Hui Li, Yuping Zhang and Haiqi Zheng *Hilbert-Huang transform and marginal spectrum for detecting and diagnosis of localized defects in roller bearings* Journal of Mechanical Technology, 2007